# CFD Analysis of Spacer Grid-Induced Cross-Flow and Vortex Structures Using URANS and DES Models

Chaehyeon Song<sup>a</sup>, Minseop Song<sup>a\*</sup>

<sup>a</sup>Department of Nuclear Engineering, Hanyang University, 222 Wangsimni Rd., Seoul, PA 04763

\*Corresponding author: <a href="hysms@hanyang.ac.kr">hysms@hanyang.ac.kr</a>

\* Keyword: Spacer grid, Cross flow, Vortex structures, URANS, DES, Q-criterion

#### 1. Introduction

The spacer grid is a key structural component in pressurized water reactors (PWRs), providing mechanical support for fuel rods while promoting coolant mixing. By enhancing heat transfer and ensuring uniform coolant distribution, spacer grids mitigate localized hot spots and potential cladding degradation. To further improve mixing, various types of mixing vanes have been developed, and in this study, a split-type vane configuration is employed.

Previous studies have primarily focused on the macroscopic thermal—hydraulic performance of spacer grids. International benchmark programs coordinated by OECD-NEA and national studies at KAERI extensively investigated the effects of mixing vanes on cross-flow mixing, pressure drop, and heat transfer enhancement. These works contributed to understanding mean flow characteristics and global performance, but did not directly address the detailed dynamics of vortical structures. This research gap highlights the necessity of explicitly characterizing vortex dynamics, which play a critical role in spacer grid performance.

However, vortices generated downstream of spacer grids are the primary drivers of subchannel mixing and downstream thermal-hydraulic performance, and their importance has been increasingly emphasized in recent experiments and numerical studies. For instance, Lu and Du [4] demonstrated through LES that large-scale vortices dominate coolant redistribution, while Dhurandhar et al. [3] reported that URANS excessively dissipates vortical motion, leading to underprediction of mixing efficiency. Thus, the predictive capability of a turbulence model is ultimately tied to its ability to faithfully reproduce vortex dynamics. This is because vortices are inherently unsteady flow structures that undergo continuous generation, development, and decay, directly governing mixing intensity and heat transfer. If a turbulence model fails to preserve such temporal fluctuations and spatial coherence, it inevitably underestimates coolant mixing and thermal performance. Therefore, vortex-resolving capability serves as a critical indicator of turbulence model accuracy.

As the need for vortex-resolved analysis has grown, various vortex identification methods have been introduced, among which the Q-criterion has been most widely used [5]. Nevertheless, most applications have remained at a qualitative level of visualization, and few

studies have directly compared turbulence models in terms of vortex structures.

The present study addresses this gap. URANS and DES simulations of spacer grid flows are performed under cold-flow conditions. The Q-criterion is applied for vortex identification, enabling a systematic comparison of URANS and DES in reproducing vortex size, spatial extent, and temporal evolution of unsteady structures. The results are expected to provide a stronger basis for turbulence model selection and contribute to CFD-based optimization of spacer grid designs.

# 2. Methodologies

## 2.1 Analysis domain and mesh

The target geometry is a spacer grid with split-type mixing vanes. At each cell intersection, two mixing vanes are installed with an inclination of 30° to the flow direction. This configuration promotes cross-flow between adjacent subchannels and generates various vortex structures downstream, improving heat transfer and reducing temperature gradients. The spacer grid geometry used in this study is shown in Fig. 1.

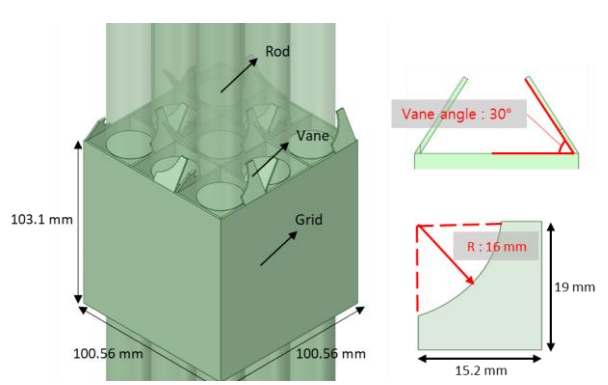


Fig 1. Geometry of spacer grid with split-type mixing vane (30° inclination)

The computational domain (Fig 2) includes the spacer grid region with upstream and downstream extensions to reduce boundary effects. A velocity inlet of 1.5 m/s and a pressure outlet (0 Pa gauge pressure) were applied, with gravity considered along the axial direction (9.81 m/s²).

To minimize entrance effects, a fully developed velocity profile obtained from a precursor simulation was imposed at the inlet, while a pressure outlet boundary condition was specified downstream. The

inherent allowance of reverse flow at the outlet ensured numerical stability, and sensitivity analyses confirmed negligible impact on the predicted wake dynamics.

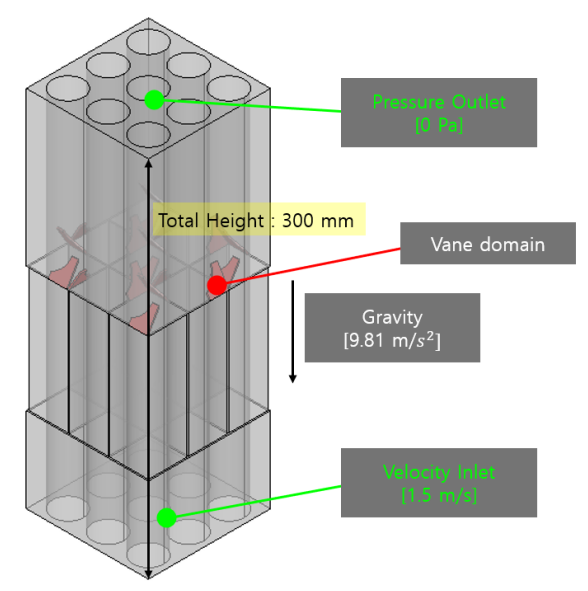
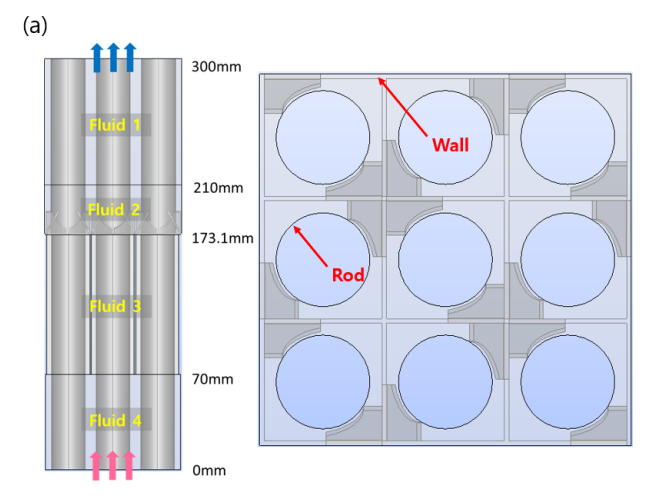


Fig 2. Computational domain of spacer grid

As illustrated in Fig. 3, the computational domain was divided into four regions (Fluid 1–4) based on local flow characteristics, with mesh generation strategies tailored to each region. For clarity, the mesh is partitioned into four regions as shown in Fig. X: Upstream Rod-Bundle Region (Fluid 4), Spacer Grid Region (Fluid 2), Vane Region (Fluid 3), and Downstream Rod-Bundle Region (Fluid 1). These region names are used consistently throughout the grid sensitivity analysis.

To ensure accurate flow resolution, structured hexahedral elements were employed in Fluids 1, 3, and 4, which have relatively simple geometries, whereas Fluid 2, containing the geometrically complex vane structures, was meshed using unstructured tetrahedral elements. In all regions, prism layers were applied along rod and wall surfaces to capture boundary layer effects, with five layers, a growth rate of 1.2, and a total thickness of 1 mm.



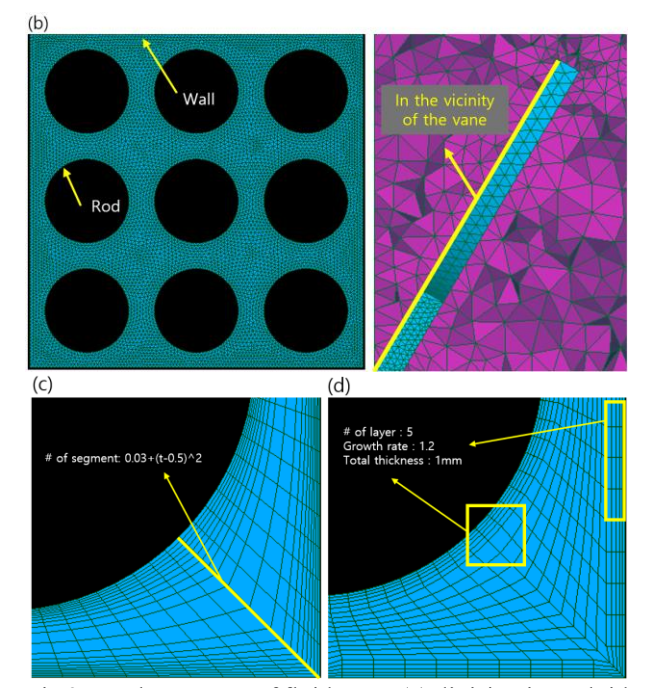


Fig 3. Mesh structure of fluid area: (a) division into Fluid 1–4, (b) Fluid 2, (c) Fluid 3, (d) Fluid 1,4

A mesh sensitivity analysis is conducted under steadystate conditions using the SST k- $\omega$  turbulence model. The computational setup is summarized in Table 1.

Table 1 : Solver settings of RANS for mesh sensitivity Analysis

schshivity Analysis		
CFD Tool	Ansys FLUENT	
Turbulence model	SST k-w	
Solver	Pressure based	
Tube wall condition	No-slip condition	
Fluid material	water	
# of time step	1,000	
Interface model	GGI	

The analysis employs four mesh conditions for steady-state grid sensitivity analysis: coarse (0.79 M cells, Fluid 3 cell size of 2.0 mm, 5 vane segments), medium (1.1 M cells, 1.5 mm, 8 vane segments), fine (1.4 M cells, 1.0 mm, 10 vane segments), and very fine (1.8 M cells, 0.5 mm, 13 vane segments), as summarized in Table 2.

Table 2 : RANS mesh information and sensitivity

Analysis

THATYSIS				
Type	Total Cells	Cell size of fluid 3	Vane segments	
	(Million)	or maid 3	segments	
Coarse	0.79	2.0 mm	5	
Medium	1.1	1.5 mm	8	
Fine	1.4	1.0 mm	10	
Very fine	1.8	0.5 mm	13	

Mesh comparison results show clear convergence trends from the fine mesh condition onward. RMS errors are 0.0829 (coarse-medium), 0.0596 (medium-fine), and 0.00606 (fine-very fine), as shown in Fig 4.

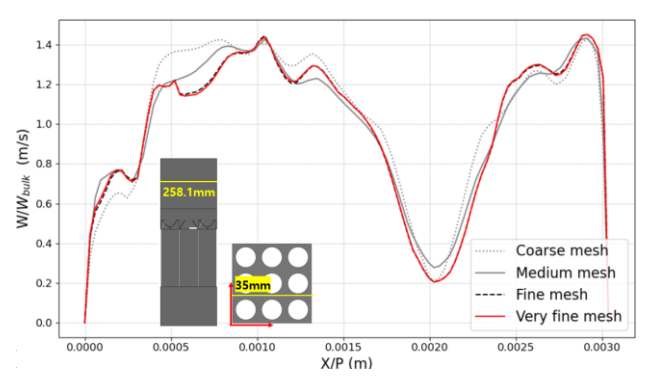


Fig 4. Mesh sensitivity results

For DES analysis, new mesh for analysis is generated using ANSYS Fluent Meshing. The LES region cell size is set to 0.7 mm, with 13 prism layers in the RANS region. The growth rate is 1.32, with a first layer thickness of 0.03 mm, last layer thickness of 0.7 mm, and total prism thickness of approximately 2.477 mm, corresponding to a boundary layer thickness of about 2.34 mm. The average y+ is maintained at 1.047, and the total cell count is approximately 15.66 million (Table 4, Fig. 5).

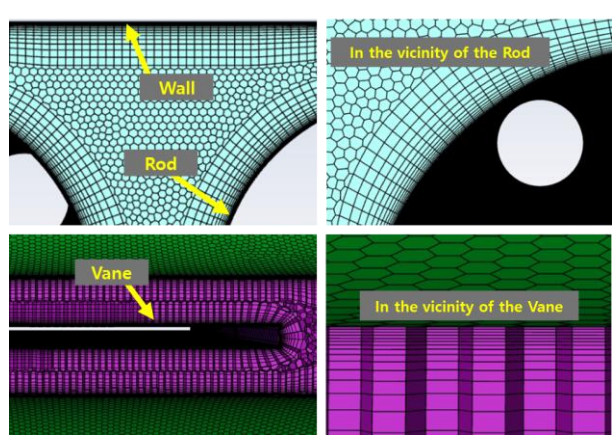


Fig 5. DES mesh structure : near wall, rod and vane region

Table 3 summarizes the detailed mesh specifications and the average  $y^+$ values used in the DES analysis.

Table 3 : DES mesh information

Tuble 5 : BEB mesh imormation		
LES region mesh size	0.7 mm	
RANS region prism	13 layers	
layers		
Growth rate	1.32	
First layer thickness	0.03 mm	
Last layer thickness	0.7 mm	
y <sup>+</sup>	1.047	
Total prism thickness	2.477 mm	
Boundary layer thickness	2.34 mm	
Total Cells (Million)	15,663,911	

Although only one DES mesh condition was finally adopted in this study, several trial simulations with coarser and finer meshes showed no significant differences in the predicted vortex structures. Based on these observations, a relatively coarse mesh was employed for the DES analysis. A more systematic grid sensitivity study will be conducted in future work to further ensure the robustness of the conclusions.

## 2.2 Parametric study set-up and solver setting

URANS simulations are performed using ANSYS FLUENT with a pressure-based solver and the SST k- $\omega$  turbulence model. The initial condition is given by the velocity distribution obtained from a simulation of fully developed steady-state flow. Transient simulations were conducted for a total physical time of 4 seconds, corresponding to 800 time steps with a time step size of 0.005 s. The computational parameters are summarized in Table 4.

DES simulations are performed under identical flow conditions, applying RANS in near-wall regions and LES in free-stream regions. To ensure fair comparison, both models used the same total simulation time of 4 seconds, number of time steps (800), and time step size ( $\Delta t = 0.005$  s). The Courant number in the DES simulation is maintained below 0.5 (Table 4)

Table 4: Solver settings of URANS and DES

	iver settings of OK	III (S WING DES
Setting	URANS	DES
CFD Tool	Ansys FLUENT	
Turbulence	SST k-w	DES (Detached
model		Eddy Simulation)
Solver	Pressure based	
Wall condition	No-slip condition	
Fluid material	water	
	(Density: 998.2 [kg/ $m^2$ ],	
	Viscocity: 0.001 [Pa·s])	
# of time step	800	
Timestep size	0.005	
Coarant	-	0.5
number		
Interface model	Nonconformal	-
	interface	
Subgrid model	-	WALE

# 2.3 Computational cost comparison

To provide a preliminary cost–accuracy perspective, the computational resources for URANS and DES were compared. Table 5 shows the wall-clock times for a 16 million-cell mesh: the URANS case (2 cores) required 4 h 37 min, while the DES case (4 cores) required 107 h. These results highlight the substantially higher cost of DES and the need for careful cost-accuracy assessment reactor-scale simulations. This comparison underscores the importance of selecting turbulence models not only based on fidelity but also considering computational feasibility for practical applications.

Table 5. Wall-clock time comparison of URANS and DES

	Core used	Wall-clock time		
URANS	2	4h 37min		
DES	4	107h		

#### 3. Results

### 3.1 CFD analysis result

Fig. 6 and Fig. 7 present a comparison of streamlines and velocity contours at t=4 s obtained from the URANS and DES simulations. The URANS results show an excessively smoothed wake in which small-scale fluctuations are suppressed, whereas the DES results reproduce more complex patterns characterized by localized vortices and mixing regions. This highlights the clear contrast between the two models in their ability to resolve unsteady wake structures.

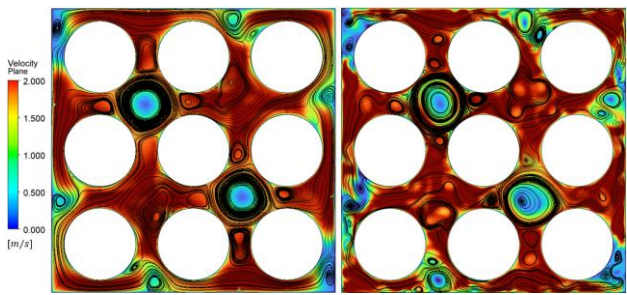


Fig 6. Streamline and contour plots at t=4 s (Top view at an axial height of 258.1 mm): comparison between URANS (left) and DES (right)

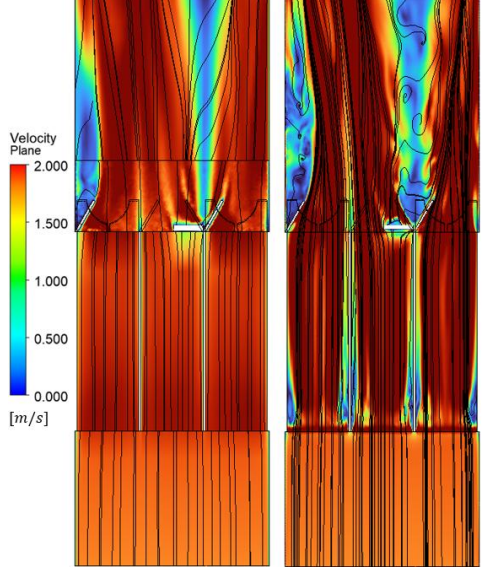
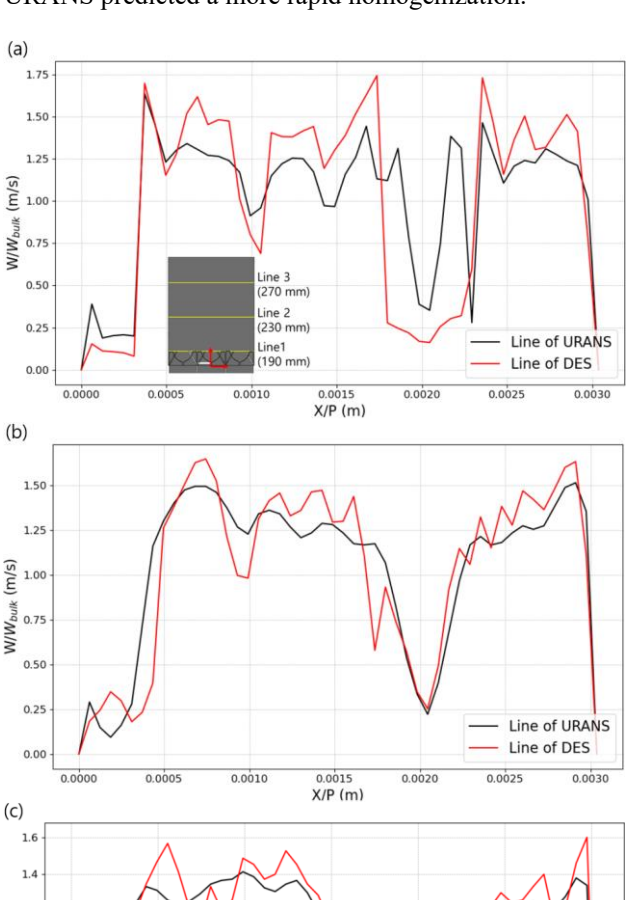


Fig 7. Streamline and contour plots at t=4 s (Side view at a radial distance of 35 mm from the central axis): comparison between URANS(left) and DES(right)

## 3.2 Comparative analysis of velocity fields

The radial sections extracted at axial heights of 190, 230, and 270 mm reveal clear differences between the

two models. In the URANS results, the high-speed core remained broad and the velocity gradients were relatively mild, yielding a more uniform distribution throughout the wake. In contrast, the DES results captured distinct high- and low-speed patches generated by jet-shear layer interactions, accompanied by steeper gradients and localized fluctuations. As the flow developed downstream, small-scale structures in DES gradually weakened but remained discernible, whereas URANS predicted a more rapid homogenization.



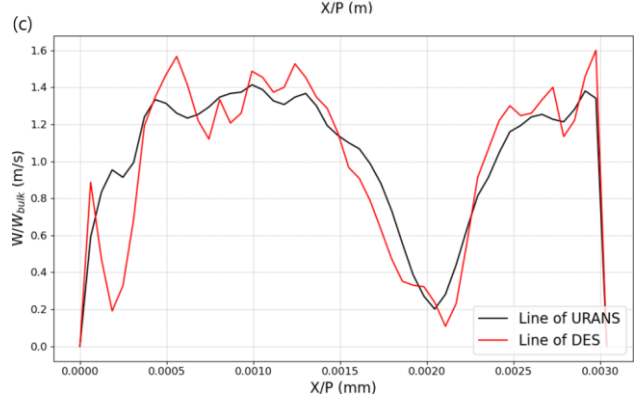


Fig 8. Radial velocity profiles along Lines 1 (a), 2 (b), 3 (c), comparing URANS and DES at t=4 s

These results suggest that DES reproduces cross-flow mixing and local shear structures with higher fidelity. The velocity distributions at the three axial locations (190, 230, and 270 mm) further highlight these differences, as shown in Fig 9. The velocity distributions at the three axial locations (190, 230, and 270 mm) further highlight these differences. URANS showed smooth and gradual variations, while DES exhibited larger peak-to-valley amplitudes and steeper gradients.

Particularly near the vane, DES captured rapid rises and drops in velocity, indicating the presence of strong shear and recirculation zones. This demonstrates that DES more accurately represents velocity fluctuations induced by vortical motion.

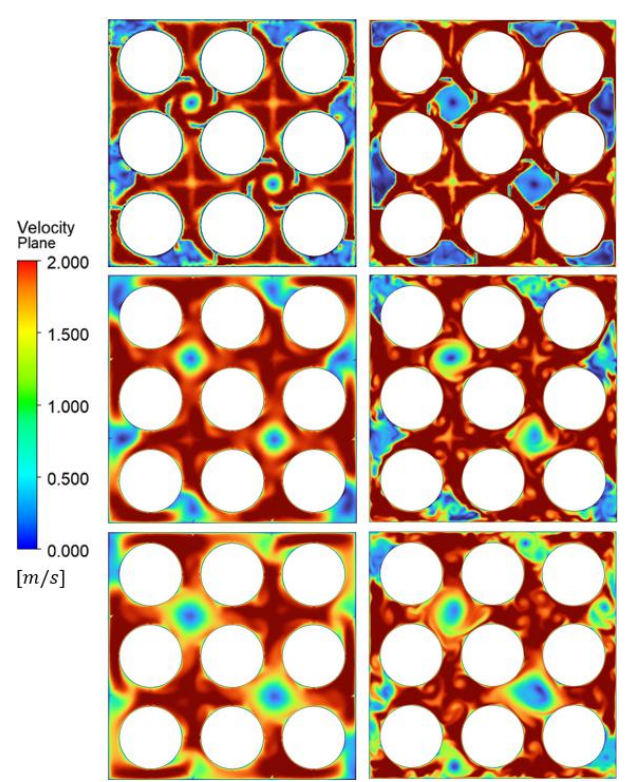


Fig 9. Velocity contours at z = 190, 230 and 270mm (from top to bottom), comparing URANS (left) and DES (right) at t=4 s

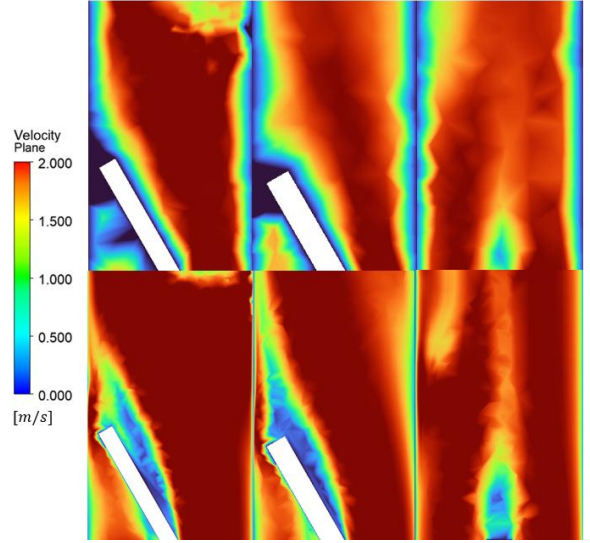


Fig 10. Axial velocity contours at r = 27, 31, 35 mm (from right to left), comparing URANS (top) and DES (bottom) at t=4 s

Axial planes were extracted at radial distances of 27, 31, and 35 mm from the central axis.

In the URANS results, the velocity field exhibited thick and smooth shear layers with monotonous distributions, reflecting over-dissipation of shear due to model averaging and numerical viscosity. In contrast, as illustrated in Fig 10, DES captured jet-like high-velocity regions originating from the vane wake and extending downstream, which gradually diffused and attenuated while maintaining localized shear structures. Such features were largely absent in the URANS results. As shown in Fig 11, URANS produced broad, smoothed peaks with mild gradients, whereas DES revealed sharper shear layers and higher peaks, more clearly resolving localized fluctuations.

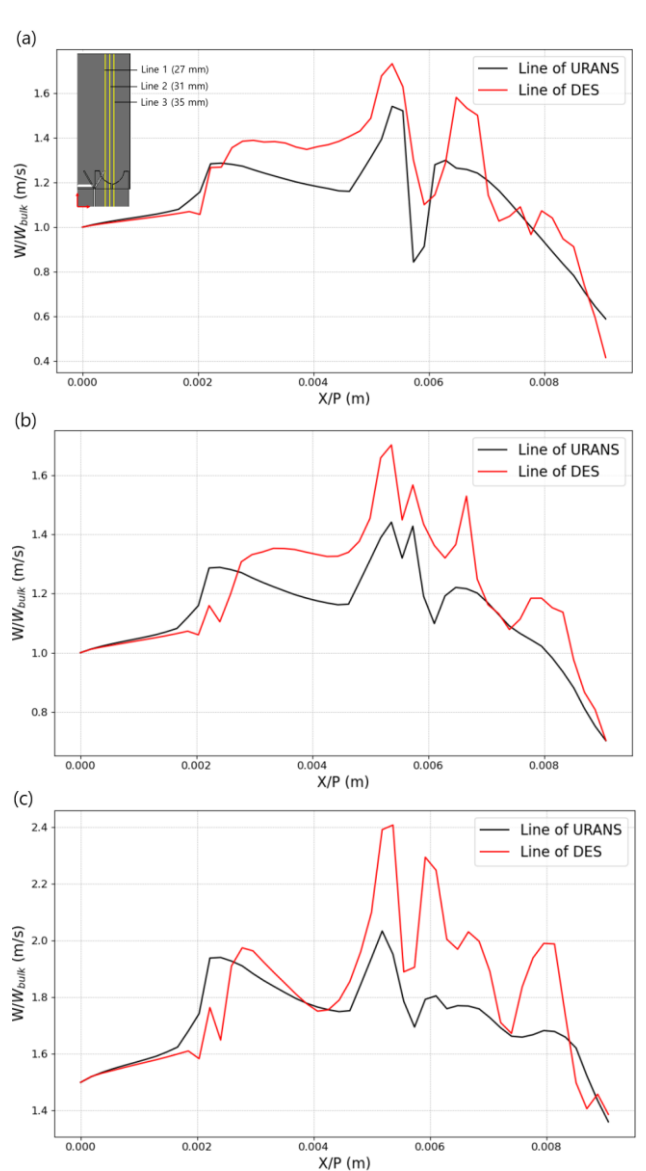


Fig 11. Axial velocity profiles along Lines 1 (a), 2 (b), 3 (c), comparing URANS and DES at t=4 s

## 3.3 Q-criterion analysis of vortex structures

The Q-criterion is applied to quantitatively compare the development and attenuation of vortices. Defined as  $Q = \frac{1}{2}(\Omega^2 - S^2)$ 

$$Q = \frac{1}{2}(\Omega^2 - S^2)$$

where  $\Omega$  is the vorticity magnitude and S is the strainrate magnitude, positive values of Q represent rotationdominated regions where vortices are present.

In this study, the Q-criterion is used to evaluate vortex dynamics downstream of the spacer grid. As illustrated in Fig. 12, six monitoring points (Point 1–6) were aligned along the central axis of the spacer grid wake, covering the region from the vane vicinity to the downstream decay zone. This configuration enabled the tracking of vortex generation, development, and dissipation throughout the wake.

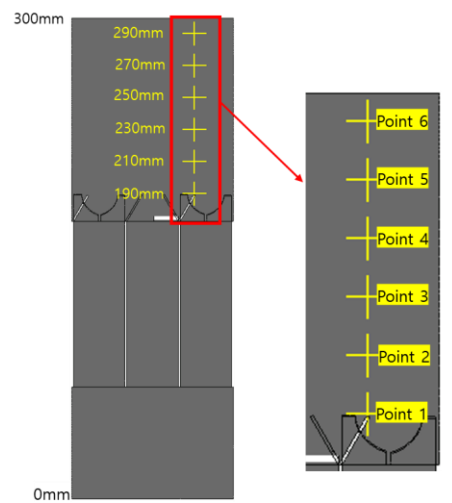


Fig 12. Location of monitoring points (Point 1–6) downstream of the spacer grid

Using the same threshold of  $Q_{th} = 10^4 s^{-2}$ , the isosurfaces clearly demonstrate that DES reproduces more extensive vortex structures compared to URANS. While the DES results capture large, continuous vortex columns extending far downstream, the URANS structures remain sparse and localized near the wake region. This indicates that DES provides a more accurate and faithful representation of vortex dynamics in terms of both spatial extent and structural coherence.

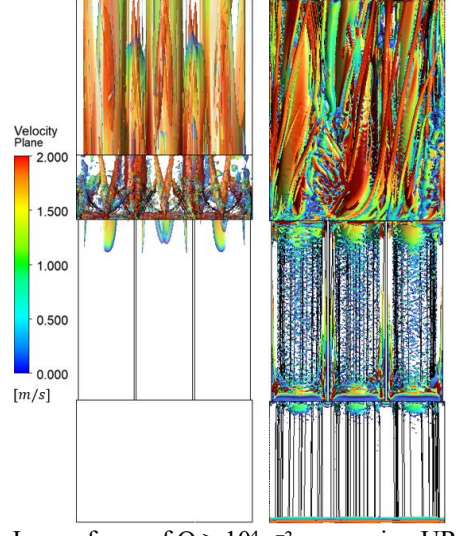


Fig 13. Iso-surfaces of Q  $> 10^4$  s<sup>-2</sup> comparing URANS and DES at t=4 s

At the representative locations, Point 1, 3, 5, the time signal revealed a clear contrast between the two models. URANS, due to its inherent averaging characteristics, exhibited only small fluctuations around zero, whereas DES showed strong oscillations alternating between positive and negative values. This indicates that DES more faithfully captured the unsteady characteristics of vortex activity.

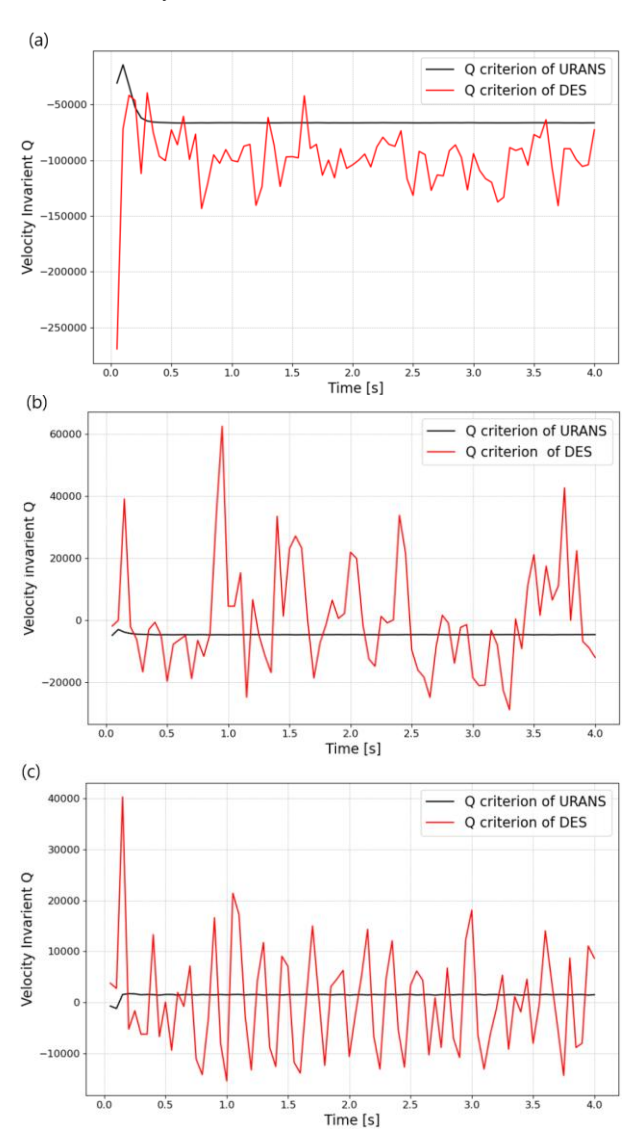


Fig 14. Time history of Q at Point 1(a), 3(b), 5(c) comparing URANS and DES

#### 4. Conclusions

In this study, CFD simulations of spacer grid wake flows were conducted using URANS and DES turbulence models. Beyond a direct comparison of flow fields, the analysis focused on vortex dynamics through Q-criterion evaluation and point-wise temporal signals. The results demonstrate that DES can sustain detailed vortex activity further downstream and preserve the unsteady characteristics of turbulence, whereas URANS tends to suppress such fluctuations due to its averaging nature. These findings emphasize that DES is more

capable of reproducing the physical processes of vortex evolution that are critical for predicting coolant mixing and temperature uniformity in fuel assemblies.

While DES provides improved fidelity, the method requires substantially higher computational effort—about 20–25 times that of URANS under the present setup. This cost gap highlights the need for strategic choices in reactor-scale simulations, such as selective application of hybrid approaches or integration with reduced-order models.

Future work will incorporate experimental validation, including PIV measurements, to confirm the numerical predictions and extend the framework toward practical guidelines for turbulence modeling in reactor thermal-hydraulic design.

#### **ACKNOWLEDGMENT**

This research was supported by the National Research Council of Science & Technology (NST) grant by the Korea government (MSIT) (No. GTL24031-000).

#### REFERENCES

- [1] P. R. Spalart, "Detached-Eddy Simulation," *Annual Review of Fluid Mechanics*, vol. 41, pp. 181–202, 2009.
- [2] R. Ranjan and D. K. Tafti, "Grid resolution assessment method for hybrid RANS-LES in turbomachinery," *International Journal of Heat and Fluid Flow*, vol. 29, no. 3, pp. 654–671, 2008.
- [3] S. K. Dhurandhar, S. L. Sinha, and S. K. Verma, "CFD analysis of effects of grid spacer vane on thermal-hydraulic performance of fluid in a 5×5 fuel channel," *Nuclear Science and Engineering*, vol. 198, no. 10, pp. 1965–1983, 2024.
- [4] C. Lu and Z. Du, "Large eddy simulation of a turbulent flow in a 5×5 rod bundle with a mixing vane spacer grid," *Frontiers in Energy Research*, vol. 12, Article 1334200, 2024.
- [5] J. Zhan, Y. Li, J. Wang, Z. He, and J. Sun, "Vortex identification and evolution of a jet in cross flow based on Rortex," *Journal of Hydrodynamics*, vol. 32, no. 5, pp. 943–954, 2020.